Paper No. 1734. (quote when citing this article)
Eleventh World Conference on Earthquake Engineering
ISBN: 0 08 042822 3

ENERGY BALANCED HYSTERESIS MODELS

B. STOJADINOVIĆ
Dept. of Civil and Env. Eng., 2380 G. G. Brown Bldg.,
University of Michigan, Ann Arbor, MI 48100-2125, USA

C. R. THEWALT
Dept. of Civil and Env. Eng., 721 Davis Hall,
University of California, Berkeley, CA 94720, USA

ABSTRACT

Hysteresis models are derived to reproduce the essential characteristics of experimentally observed flexural behavior for reinforced concrete elements. They are computationally inexpensive and versatile. As such, hysteresis models are often used to model the behavior of reinforced concrete structural elements for global nonlinear analysis of structures.

A pair of of new piecewise linear Energy Balanced models are proposed. The new models are based on controlling the amount of dissipated hysteretic energy and the rate of stiffness degradation observed in experiments. The Energy Balanced models are compared to six well-known piecewise linear hysteresis models to examine the differences in the shapes of hysteresis loops, the stiffnesses of loop segments and the amount of dissipated hysteretic energy. The comparison shows that the new Energy Balanced models are capable of accurately reproducing the energy dissipation and stiffness degradation observed in experiments.

KEYWORDS

Hysteresis model, Reinforced concrete, Energy dissipation, Stiffness degradation, Computer implementation

INTRODUCTION

Many computational models have been developed to capture the nonlinear behavior of reinforced concrete beam-column elements. The models can be classified into three classes: (1) models is based on two-dimensional or three-dimensional finite element discretization; (2) models derived from the fiber discretization of the cross section and element assembly using the filament or the variable stiffness formulation; (3) hysteresis models.

The reinforced concrete hysteresis models are empirically based. The goal of the modeling process is to represent the most essential properties of the behavior observed in the experiments on beams and columns under quasi-static cyclic loading. Hysteresis models prescribe a set of rules governing the

behavior of the model under all possible cyclic loading histories.

An efficient analysis of large reinforced concrete frame structures requires a computationally inexpensive and acceptably accurate model for the most common structural elements or sub-systems. The hysteresis models are good candidates to fulfill this role. Therefore, in order to facilitate a seismic analysis of the elevated freeway structure [Stojadinović 95], a set of reinforced concrete hysteresis models was used to represent the experimentally observed behavior of upgraded bridge outrigger knee joints.

Six existing reinforced concrete hysteresis models are reviewed. A pair of new hysteresis models, based on controlling the amount of dissipated hysteretic energy and the rate of stiffness degradation, are proposed and implemented. All eight models are evaluated by comparing the shape of the hysteresis loops, the degradation of characteristic loop stiffnesses and the energy dissipation rates to the measurements obtained from the experiments on upgraded outrigger knee joints [Thewalt 92]. The evaluation shows that simple hysteresis models can be enhanced, at the expense of little computational effort, to accurately reproduce the measured stiffness degradation and energy dissipation of reinforced concrete structural elements.

HYSTERESIS MODELS

A reinforced concrete hysteresis model defines a monotonic force/deformation response envelope and a set of rules for constructing the hysteresis loops. The monotonic response envelope is usually symmetric about the origin. The hysteresis loop rules define the behavior of the model in the event of unloading from the response envelope, cycling within the hysteresis loop and reloading to the response envelope. Depending on the types of functions used in the rules, the hysteresis models can be curvilinear or piecewise linear.

Six well-know piecewise linear hysteresis models are considered (Figure 1). The simplest model is the bi-linear (elastic-plastic) hysteresis model. Clough hysteresis model [Clough 66] improves on the bi-linear model by considering the degradation of the hysteresis loop stiffness. Takeda model [Takeda 70, Otani 74] improves on the Clough model in two ways. The monotonic response envelope is tri-linear, accounting for the event of cracking. The unloading stiffness K_u is a fraction of the elastic stiffness K_y that degrades exponentially with increasing deformation ductility μ:

$$K_u = K_y \, \mu^{-0.5}. \tag{1}$$

The Q-hyst model [Saiidi 82] merges the simplicity of the Clough model with the unloading stiffness degradation feature of the Takeda model. Another modification of the Takeda model was implemented in IDARC [Kunnath 92]. Degradation of the unloading stiffness was modeled by adopting a common focal point for all unloading segments of the hysteresis loops. The sixth hysteresis model, developed in [Mander 84], generalizes upon the previous models. It features a tri-linear response envelope and a hysteresis loop composed of two tri-linear halves. By varying two model parameters, Mander hysteresis model is capable of simulating all of the previous mentioned models except the IDARC model.

PROPOSED ENERGY BALANCED MODELS

The proposed reinforced concrete hysteresis models are based on empirical observations and are piecewise linear. Both models have a symmetric multi-segment response envelope. The segments are defined by the first-crack, yield, ultimate-resistance and failure events to match the experimentally observed response envelope. Both models have hysteresis loops consisting of two halves, symmetric about the origin of the coordinate system. The proposed models differ in the hysteresis loop construction rules: the hysteresis loops of the Bi-Linear Energy and Tri-Linear Energy Balanced models are made up of bi-linear and tri-linear symmetric halves, respectively (Figure 2). The length and stiffness of the loop segments are determined to match the observed stiffness degradation rates as well as the measured energy dissipation.

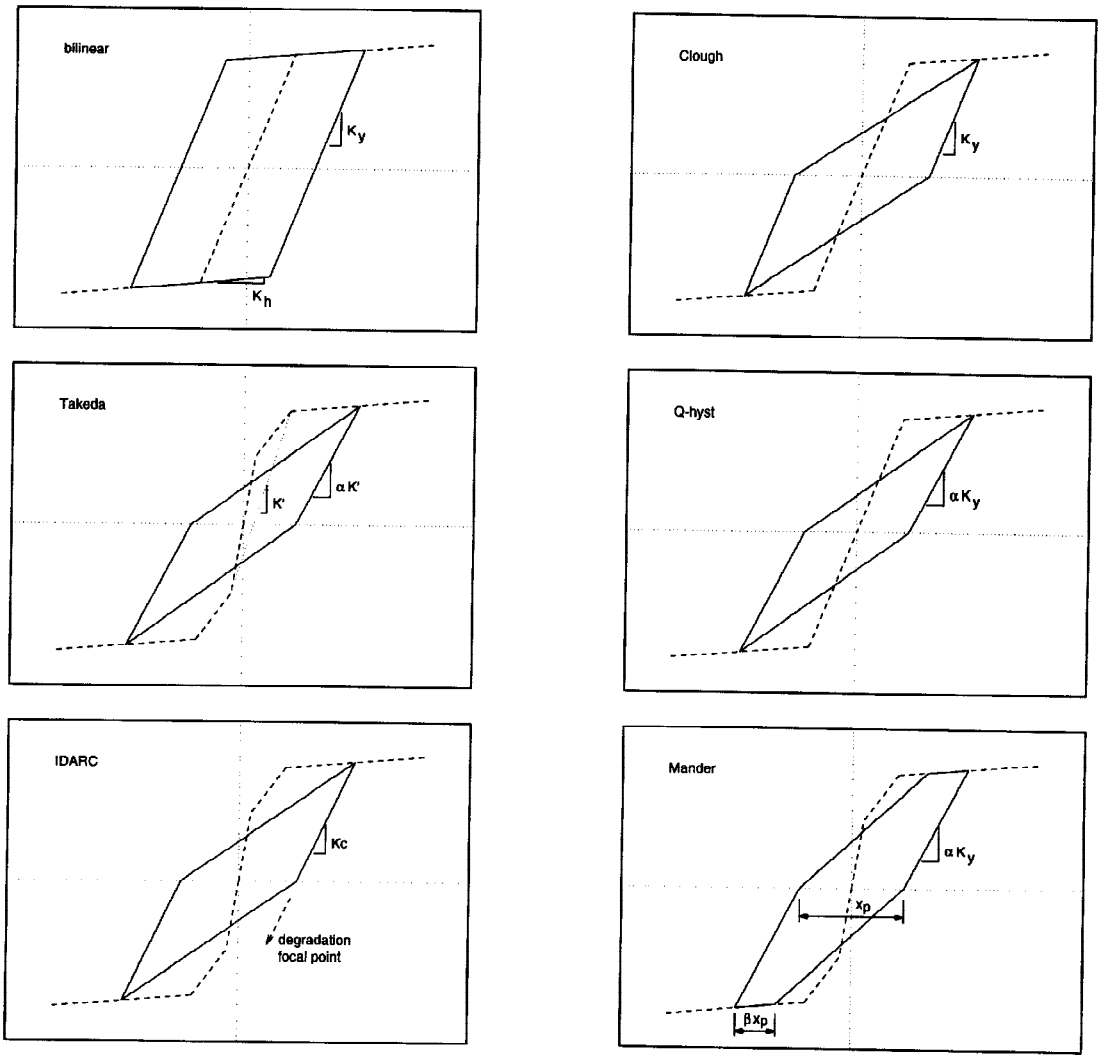

Figure 1: Well-known piecewise linear hysteresis models.

Definition of the Energy Balanced Model

The experimental data used to calibrate the Energy Balanced models in this study was obtained from a series of tests conducted on upgraded outrigger knee joint sub-systems [Thewalt 95]. The upgraded specimens were designed to develop a plastic hinge in the column. Therefore, the measured force/displacement response of the specimen is representative of a reinforced concrete element responding predominantly in flexure.

The force/displacement response of an upgraded specimen is shown in Figure 3. The events of first cracking, yielding of longitudinal reinforcement, ultimate capacity and failure are easy to identify on the specimen response envelope. First yielding of column longitudinal reinforcement occurred at a displacement of 1.25 cm. The force/displacement hysteresis loops are well-rounded, providing significant energy dissipation and showing no pinching up to a displacement of 10 cm, corresponding to a tip displacement ductility of 8. The measured loops are roughly symmetric about the coordinate system origin.

The shape of a hysteresis loops can be quantified by the slopes measured at several characteristic points of the loop Figure 3). The unloading segment can be defined by the tangent unloading stiffness K_u or the average unloading stiffness $\overline{K}_u$ [Krawinkler 92]. The reloading segment of the loop is best described by the slope at the point of zero displacement, the tangent zero-displacement stiffness K_z. The loop ends at a slope similar to the hardening stiffness of the response envelope K_h. The three characteristic

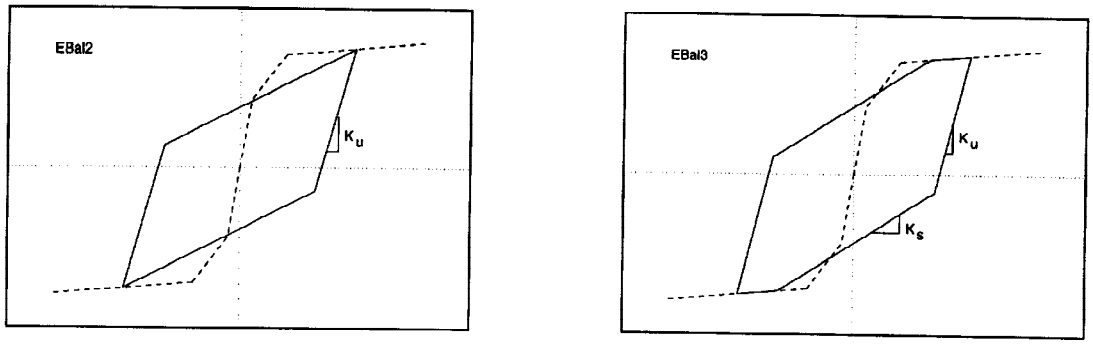

Figure 2: Energy Balanced models.

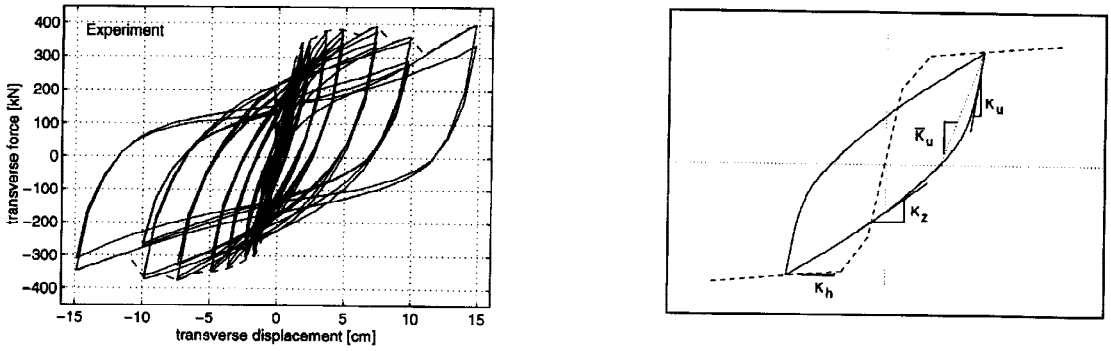

Figure 3: (a) Force/displacement response. (b) Characteristic stiffnesses of a hysteresis loop.

stiffnesses were measured during each load cycle applied to the three outrigger knee joint specimens. The stiffness values, normalized with respect to the specimen yield stiffness, are plotted as a function of the tip displacement ductility in Figure 4. The stiffnesses degrade considerably with increasing ductility. The measured values were interpolated as:

$$K_u = 1.6\, K_y \mu^{-0.35} \tag{2}$$

$$\overline{K}_u = 1.0\, K_y \mu^{-0.3} \tag{3}$$

$$K_z = 0.5\, K_y \mu^{-0.6}. \tag{4}$$

The values of the coefficients are representative of a well-confined square column responding in flexure. Further study is needed to establish a range of coefficient values appropriate for different structural systems.

Another important measure of the hysteresis response is the dissipated hysteretic energy, quantified using an equivalent viscous damping ratio δ. The change of the equivalent viscous damping ratios observed during the tests of three knee joint specimens is shown in Figure 4. The damping ratios remain at approximately 5% during the pre-yield load cycles. After yielding, the ratios grow to peak values of approximately 25% at a displacement level where the specimens reach their ultimate capacity. The measured damping values were interpolated in the least squares sense using a parabola:

$$\delta = \begin{cases} 0.047 & \text{if } \mu < 1 \\ -0.004\mu^2 + 0.071\mu - 0.02 & \text{otherwise.} \end{cases} \tag{5}$$

The use of the interpolation formulas in the Energy Balanced models is illustrated using the Bi-Linear model. The stiffness of the unloading segment is set equal to the average unloading stiffness $\overline{K}_u$ (Equation 3). The end-point of the reloading segment is computed to preserve the central symmetry of the hysteresis loop with respect to the coordinate system origin. The end-point of the unloading segment and, implicitly, the stiffness of the reloading segment, are computed to insure that the area of the hysteresis loop conforms to the energy dissipation model defined by Equation 5. The area of the triangle in

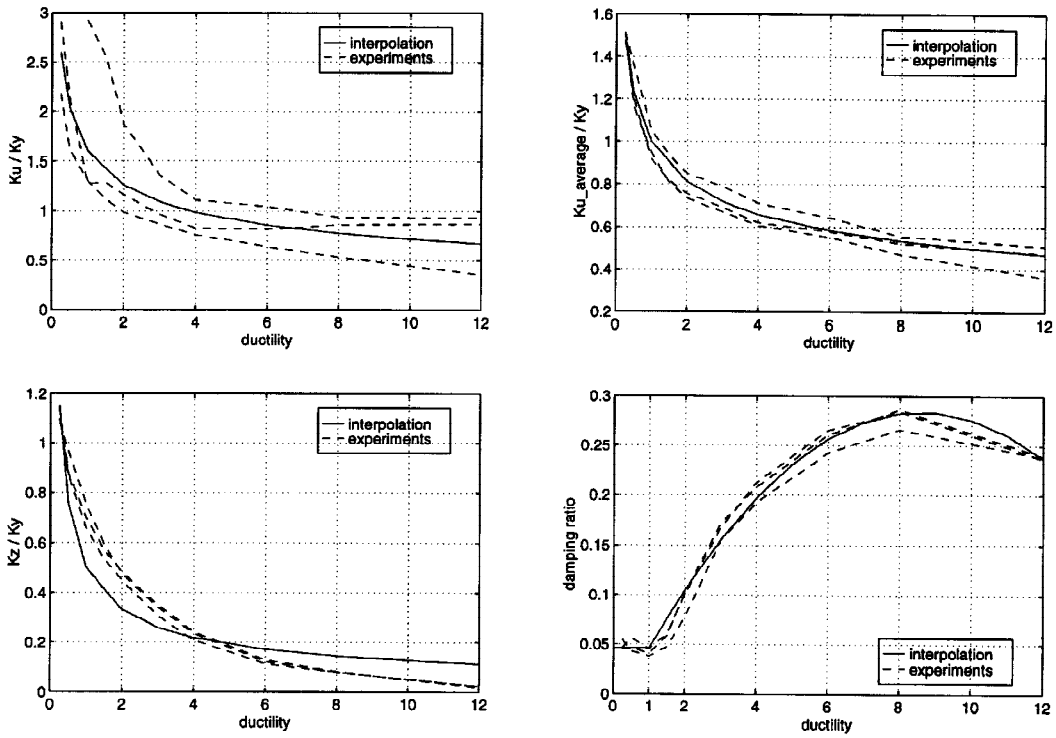

Figure 4: Interpolation of the measured stiffness degradation rates and equivalent viscous damping.

Figure 5 is equal to one half of the area of the hysteresis loop A_h, computed from the equivalent viscous damping interpolation. The following angles are then calculated:

$$\alpha = \arctan(K_u); \qquad \tau = \arctan(K_{pp}). \tag{6}$$

Given the length of the peak-to-peak diagonal D_{pp} and the angle $(\alpha - \tau)$, the length of the projection of the unloading segment on the displacement axis is

$$\Delta = \frac{A_h}{D_{pp}\,\sin(\alpha - \tau)}\,\cos\alpha. \tag{7}$$

The end-point of the unloading segment is defined by the coordinates

$$d_1 = d - \Delta \tag{8}$$

$$F_1 = F - K_u\Delta. \tag{9}$$

COMPARISON OF HYSTERESIS MODELS

The measured force/displacement responses of the upgraded outrigger specimens are used as a benchmark to compare the performance of the hysteresis models (Figure 7). The envelopes of the models were computed to give the best possible estimate of the measured response envelope. The models are subjected to a displacement history that mimics the displacement history imposed on the specimen.

The Bi-linear model poorly represent the hysteresis behavior of a reinforced concrete elements. The importance of stiffness degradation, introduced in the Clough model, to closely model the reinforced concrete hysteresis response is evident from the response graphs. Degradation of unloading stiffness with increasing ductility, introduced in the Takeda model, gives an even more realistic model response. The model with three-segment half-loops, the Mander and the Tri-Linear Energy Balanced models, reproduce the measured response hysteresis loops very closely at all ductility levels.

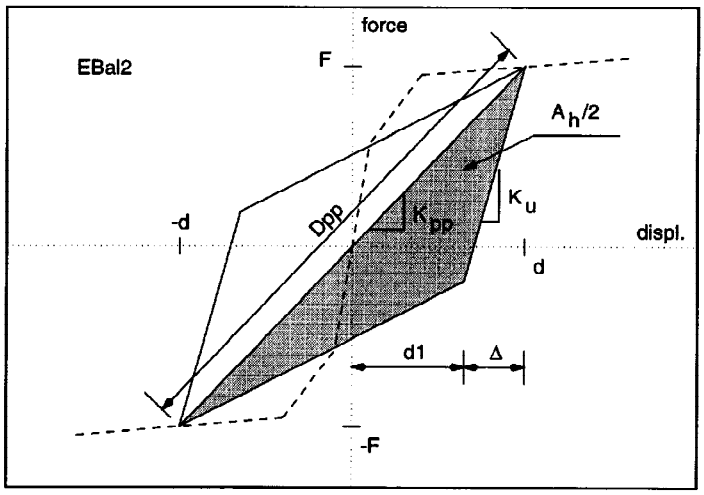

Figure 5: Construction of the hysteresis loop for the Bilinear Energy Balanced model.

Unloading stiffnesses of the hysteresis loop models are compared to the test measurements on the three upgraded knee joint specimens in Figure 6. The Bi-linear and the Clough model have a constant unloading stiffness, equal to the model yield stiffness. All other models incorporate exponential unloading stiffness degradation. The difference in degradation rates is caused by the different ductility exponent values used in the models.

The energy dissipation characteristics of the models are compared by plotting the equivalent viscous damping ratios with respect to the displacement ductility (Figure 6) and comparing them to the measured damping ratios. The Bi-linear model grossly overestimates the energy dissipated in the specimens. The IDARC model has a constant damping ratio of approximately 20% for all ductility levels. Energy dissipated in loops generated by the remaining models increases with increasing ductility, following the basic trend observed in the experiments. The Clough model slightly overestimates damping, while Takeda, Q-hyst and Mander models underestimate damping throughout the range of ductilities. Damping does not decrease in the post-ultimate ductility range for these four models. On the other hand, both Energy Balanced models are designed to closely follow the experimental data.

The Energy Balanced models require more computational effort than the other hysteresis models. The Bi-Linear and the Tri-Linear Energy Balanced models were 1.9 and 3.1 times slower than the Clough model, while Mander's model was only 1.5 times slower. However, if some parameters are pre-calculated the cost of using the Energy Balanced models becomes acceptable. For example, the simplified Bi-Linear Energy Balanced model was only 19% slower than the Clough model.

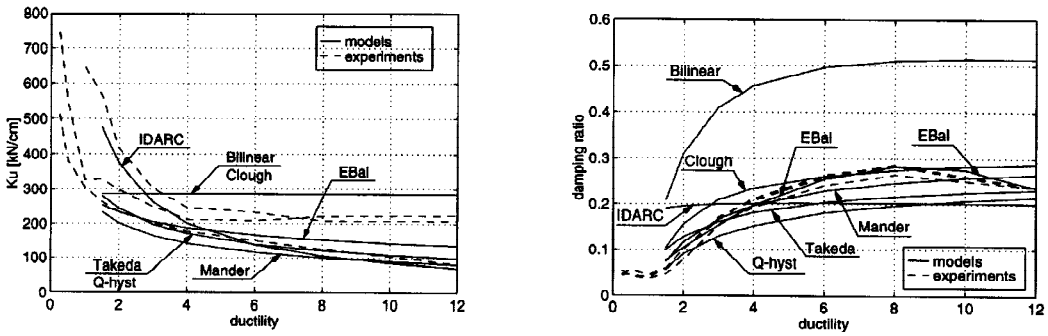

Figure 6: Comparison of model unloading stiffness degradation rates and energy dissipation.

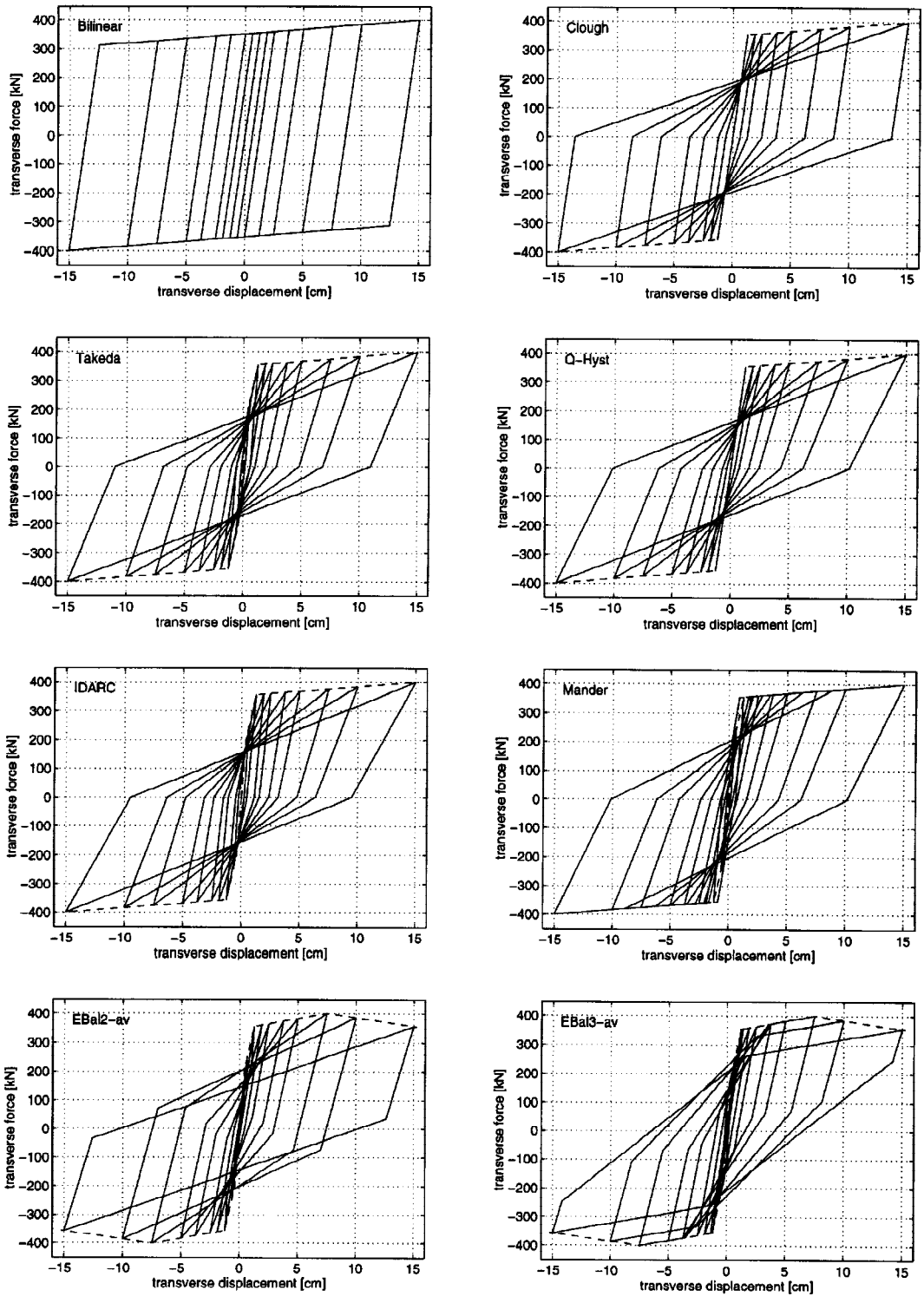

Figure 7: Force/displacement response of the models.

CONCLUSION

Two Energy Balanced hysteresis models, based on quantifying the amount of dissipated hysteretic energy and the rate of stiffness degradation, were proposed and implemented. The comparison of these models to the experimentally obtained data shows that the new models match the observed response. The evaluation of the hysteresis models demonstrates the subtle differences among the models.

The Energy Balanced models are designed to be general tools for global analysis of structures. The parameters of the model envelope, the stiffness degradation rates and the energy dissipation function can be determined using a wider sample of experimental data or from data computed by more sophisticated analytical models. Once the model parameters are established, the Energy Balanced models are good candidates for use in performance based earthquake-resistant design procedures.

REFERENCES

[Clough 66] R. W. Clough. "Effect of stiffness degradation on earthquake ductility requirements." Technical Report SESM 66-16, Department of Civil Engineering, University of California, Berkeley CA 94720, 1966.

[Krawinkler 92] H. Krawinkler. "Guidelines for cyclic seismic testing of components of steel structures." Technical Report ATC-24, Applied Technology Council, 1992.

[Kunnath 92] S. K. Kunnath, A. M. Reinhorn, and R. F. Lobo. "A program for the inelastic damage analysis of reinforced concrete structures." Technical Report NCEER-92-0022, NCEER, SUNY, Buffalo, NY 14261, 1992.

[Mander 84] J. B. Mander, M. J. N. Priestley, and R. Park. "Seismic design of bridge piers." Technical Report 84-2, Department of Civil Engineering, University of Canterbury, Christchurch, New Zealand, 1984.

[Otani 74] S. Otani. "SAKE: A computer program for inelastic response of R/C frames to earthquakes." Technical Report SRS/413, University of Illinois at Urbana-Champaign, 1974.

[Saiidi 82] M. Saiidi. "Hysteresis models for reinforced concrete." *Journal of ASCE, Structural Engineering Division*, 108(ST5):1077–1087, 1982.

[Stojadinović 95] B. Stojadinović and C. R. Thewalt. "Upgrading bridge outrigger knee joint systems." Technical Report UCB/EERC–95/03, Earthquake Engineering Research Center, University of California, Berkeley CA 94720, 1995.

[Takeda 70] T. Takeda, M. A. Sozen, and N. N. Nielsen. "Reinforced concrete response to simulated earthquakes." *Journal of ASCE, Structural Engineering Division*, 96(ST12):2557–2573, 1970.

[Thewalt 92] C. R. Thewalt and B. Stojadinović. "Behavior and retrofit of bridge outrigger beams." In *Proceedings, 10th WCEE*, pages 5291–5296, Madrid, Spain, 1992.

[Thewalt 95] C. R. Thewalt and B. Stojadinović. "Behavior of bridge outrigger knee joint systems." *Earthquake Spectra*, 11(3):477–509, 1995.